Coordination to a Di-*tert*-butylphosphidoboratabenzene Ligand with Electronically Unsaturated Group 10 Transition Metals

Bret B. Macha[1], *Josée Boudreau*[1], *Laurent Maron*[2], *Thierry Maris*,[3] *and Frédéric-Georges Fontaine*[1]*

[1]Université Laval, Faculté des Sciences et de Génie, Département de Chimie

1045 Avenue de la Médecine, Pavillon Alexandre-Vachon

Cité Universitaire, Québec, Qc, Canada, G1V 0A6

[2]Université de Toulouse, INSA, UPS, LPCNO

135 avenue de Rangeuil, Toulouse, France, 31077

[3] Département de Chimie, Université de Montréal, Montréal, Québec H3C 3J7, Canada

E-mail: frederic.fontaine@chm.ulaval.ca

This is the peer reviewed version of the following article: [Coordination to a Di-tert-butylphosphidoboratabenzene Ligand with Electronically Unsaturated Group 10 Transition Metals, Organometallics 2012, 31, 6428−6437], which has been published in final form at [10.1021/om300668u].

Table of Contents Graphic

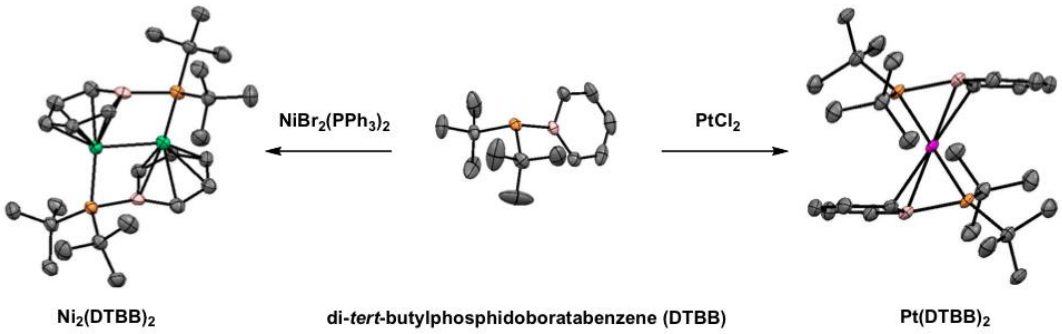

Synopsis

The di-*tert*-butylphosphidoboratabenzene $[DTBB]^-$ species was synthesized and coordinated to nickel(II) and platinum(II). In the former case, the DTBB ligand binds one nickel center by the boratabenzene moiety and bridges the another center through the phosphorus atom, while in the later case the DTBB binds in a allylic fashion by the $R_2P\text{-}BR{=}CR_2^-$ moiety.

Abstract

A new boratabenzene-phosphine ligand, di-*tert*-butylphosphidoboratabenzene [DTBB]$^-$, has successfully been synthesized by reduction of the corresponding di-*tert*-butylchlorophospidoborabenzene compound (**2**). The species was structurally characterized with both K^+ (**3**) and 18-crown-6.K^+ (**4**) as counterions. Reactions of two equivalents of di-*tert*-butylphosphidoboratabenzene with $NiBr_2(PPh_3)_2$, $PtCl_2$, and $PtCl_2$(COD) were undertaken and were successful in yielding three new organometallic boratabenzene species, (μ-κ-η^6-$C_5H_5BP(tBu)_2)_2Ni_2$ (**5**), (η^3-(C,B,P)-$C_5H_5BP(tBu)_2)_2Pt$ (**6**), and (η^3-(C,B,P)-$C_5H_5BP(tBu)_2$)(κ-$C_8H_{12}(P(tBu)_2BC_5H_5)Pt$ (**7**), respectively. The di-*tert*-butylphosphidoboratabenzene species displays remarkable tendency to coordinate to transition metal species in two distinct modes closely associated with other reported boratabenzene and allyl-like interactions. Also of interest is the ability for di-*tert*-butylphosphidoboratabenzene to be able to coordinate within monomeric as well as dimeric transition metal compounds. The synthesis and characterization will be discussed in detail along with DFT calculations in order to validate these research findings.

Introduction

Borabenzene (I, Chart 1) and boratabenzene (II, Chart 1) are 6 π-electron aromatic analogues of the respective familiar benzene and cyclopentadienyl ring systems displaying boron substitution for one of the carbon atoms.[1] Derivatives and metal complexes involving these ligands have been playing prominent roles in a large array of applications, most notably as catalysts[2] and for their inherent optoelectronic properties.[3] The coordination chemistry of boratabenzene has been widely explored, but is traditionally limited to simple interactions of the heteroaromatic π-system with transition metals (III, Chart 1). These interactions can be readily predictable due to their close chemical resemblance to cyclopentadienyl ligand scaffolds, with a few notable exceptions of species coordinated to formal d^0 transition metals resulting in "ring-slippage" from the perfectly symmetric η^6 coordination of the boratabenzene to an η^5 coordination where the boron-metal distance is observed to be longer than the carbon-metal distances (IV, Chart 1).[4]

There are two noteworthy examples of a boratabenzene moiety displayed within the coordination sphere of a transition metal complex with the anionic π-system completely sequestered from the metal center. In 2009, our research group reported a chloroboratabenzene species where the anionic moiety binds to the electrophilic platinum core through a Pt-Cl-B interaction (V, Chart 1).[5] The steric bulk of the two N-heterocyclic ligands bound to platinum inhibits coordination of the heteroaromatic ring onto the metal center. It has recently been observed that the dissociation of the chloroboratobenzene anion is possible with the presence of a Lewis base.[6] The other example is the diphenylphosphidoboratabenzene $[DPB]^-$ anion synthesized by Fu in 1996 that serves as an anionic analogue of the ubiquitous triphenylphosphine ligand (VI, Chart 1) .[7] Utilizing this $[DPB]^-$ ligand the Fu group was able to synthesize complexes of zirconium(IV), iron(II), and rhodium(I), as examples of the wide applicability for this phosphine

to coordinate in the same manner regardless of both the metal and the oxidation state of the final complex. However, these complexes reported by Fu are electronically saturated $18e^-$ complexes, with the exception of a $16e^-$ rhodium square-planar species. The behavior and coordination of the phosphidoboratabenzene ligands with electronically unsaturated transition metal species was never probed and could possibly lead to coordination in an alternative manner as of yet not observed. In our exploration of novel coordination modes for borabenzene and boratabenzene, we were interested in investigating the coordination chemistry of phosphidoboratabenzene molecules, notably with electronically unsaturated metal precursors. The interest for this project lies in the possibility of generating highly electron-rich, unsaturated transition metal species that could react with increasingly unactivated substrates. Towards this aim, we have synthesized a di-*tert*-butylphosphidoboratabenzene $[DTBB]^-$ ligand (VII, Chart 1) and have looked at its coordination to nickel(II) and platinum(II) precursors. The experimental characterization of the novel species and the DFT modeling of the interactions between phosphidoboratabenzene and the group 10 metals are presented herein.

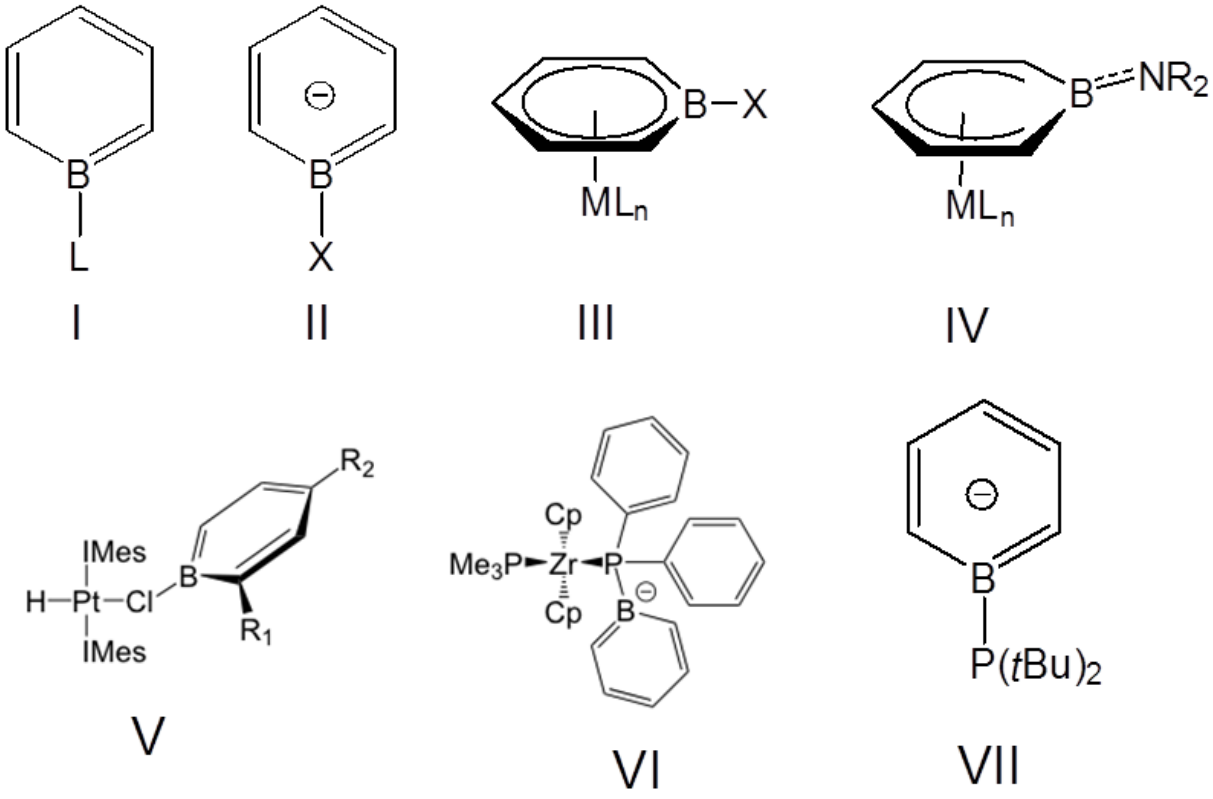

Chart 1. Various types of bora(ta)benzene and boratabenzene complexes. L is a neutral 2-electron donor and X is an anionic 2-electron donor.

Results and Discussion

Theoretical investigation of the coordination of the phosphidoboratabenzene

The possibility for the diphenylphosphidoboratabenzene $[DPB]^-$ to bind to a metal center by the phosphorus moiety is directly due to the inherent nature of the P-B interaction, which disfavors orbital overlap between the lone pair of electrons on the phosphorus atom with the p_z orbital on boron.[8] Indeed, the boratabenzene-phosphido interaction crystallographically displays this tetrahedral geometry at the phosphorus center whereas the boratabenzene-amido interaction

yields a trigonal-planar nitrogen center. Although the $[DPB]^-$ ligand synthesized by Fu was experimentally shown to be an exceptionally strong electron donating phosphine due to the presence of the anionic charge on the boratabenzene moiety,[9] it could be possible to increase its Lewis basicity by having alkyl groups rather than electron withdrawing phenyl groups. Theoretical modeling of the phosphidoboratabenzene moiety's interaction with transition metals has never been reported, so DFT calculations were conducted on the di-*tert*-butylphosphidoboratabenzene $[DTBB]^-$ ligand as well as the $[DPB]^-$ ligand synthesized by Fu to compare the electron donating properties of these two species.

The first thing that can be observed from the results obtained using DFT calculations (MPW1PW91 functional 6-311+G(2d) (Ni) 6-311+G(d,p) (C, H, B, O, P)) is that the HOMO level of the $[DPB]^-$ is centered on the 6-electron π-system and is equivalent to the e_{1g} orbital of benzene (Figure 1). The lone pair on the phosphorus atom is present as the HOMO-1, but at 20.7 $kcal.mol^{-1}$ lower in energy than the HOMO. For the $[DTBB]^-$, the same trend was observed, but the difference in energy between the HOMO and HOMO-1 was reduced to 11.3 $kcal.mol^{-1}$, which can be attributed to the greater donating ability of the *tert*-butyl substituents compared to phenyl substituents.

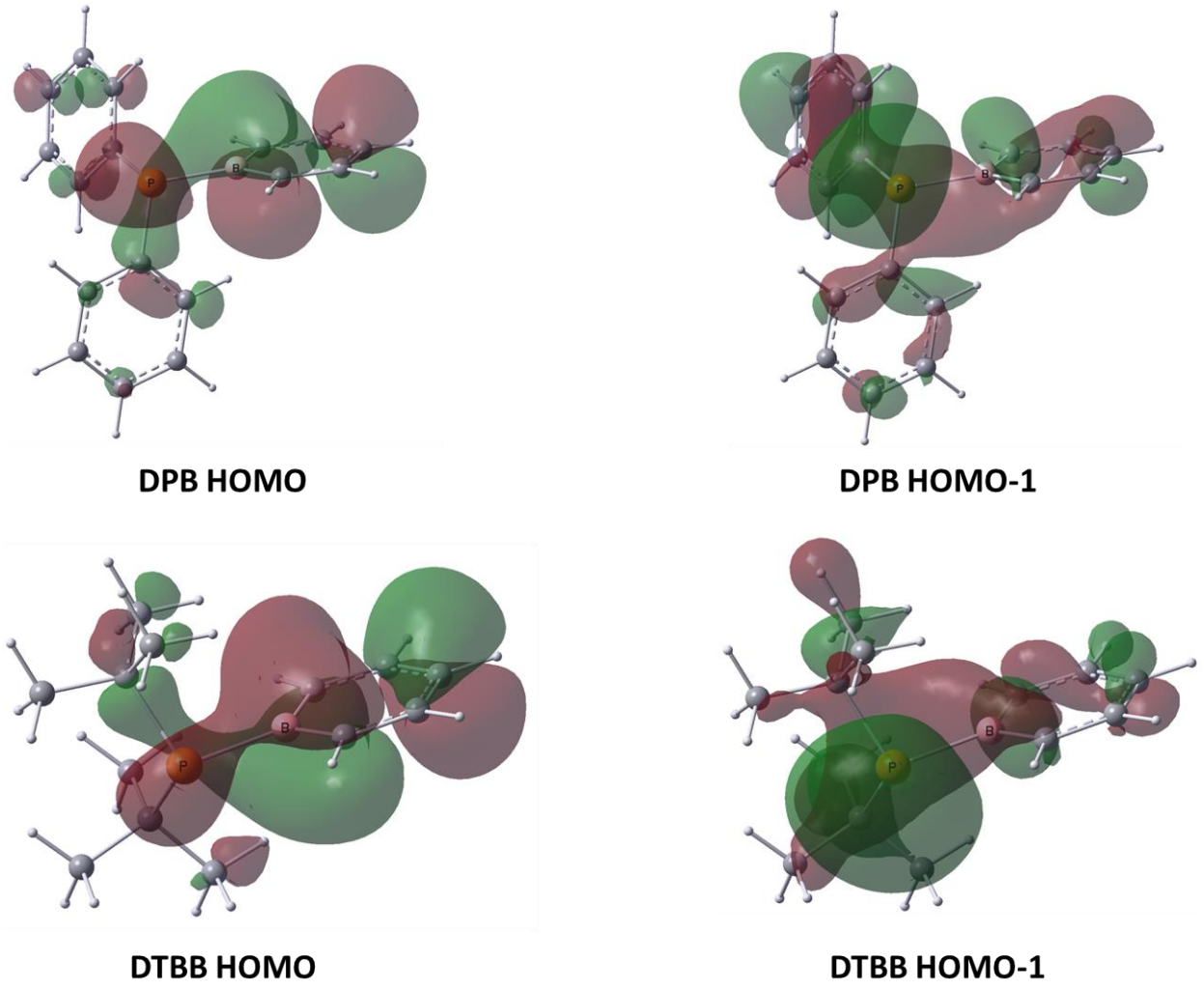

Figure 1. HOMO and HOMO-1 orbital representations for $[DTBB]^-$ and $[DPB]^-$ as determined using DFT.

Using the A1 carbonyl stretching frequency of model complexes LNi(CO)$_3$ as an indicator of the electron donating capability of ligands L,[10] $[DPB]^-$ as well as designed $[DTBB]^-$ species were compared against several phosphines as well as N-heterocyclic carbenes (Table 1). The model compound $[(CO)_3Ni(DPB)]^-$, where the $[DPB]^-$ ligand is bound to nickel only by the phosphorus moiety, was calculated to have a ν_{CO} stretching frequency of 2035.3 cm^{-1}, 32 cm^{-1} lower in frequency than $[(CO)_3Ni(PPh_3)]$.[10] This energy difference is less radical than what was

observed by Fu for the $CpFe(CO)_2(DPB)$ species, which was observed to shift the resonance 43 cm^{-1} lower in frequency than $[CpFe(CO)_2(PPh_3)]^+$.[7] However, there is no doubt that the donating capability of $[DTBB]^-$ is greatly enhanced vis-a-vis $[DPB]^-$. With a predicted ν_{CO} stretching frequency of 2026 cm^{-1}, the $[DTBB]^-$ resonance is 20 cm^{-1} lower in energy than even the most donating carbenes.

Table 1. A few selected ν_{CO} stretching frequencies of CO bonds in $LNi(CO)_3$ complexes of phosphine and carbene ligands compared to the DFT results for $[DTBB]^-$. Gaussian 03 MPW1PW91 functional 6-311+G(2d) (Ni) 6-311+G(d,p) (C, H, B, O, P). Calculated values have been corrected according to function Exp = Calc*0.9540.[10]

	Stretching Frequencies (cm^{-1})	
Ligand	**Calculated**	**Experimental**
PF_3	2111.3	2110.8
PPh_3	2067.5	2068.9
$P(tBu)_3$	2055.3	2056.1
ICy	2049.8	2049.6
$[DPB]^-$	2035.3	-
$[DTBB]^-$	2026.4	-

Synthesis of $K^+[DTBB]^-$

Synthesis of di-*tert*-butylphosphidoboratabenzene ($[DTBB]^-$) was carried out by first synthesizing the neutral borabenzene-phosphine adduct di-*tert*-butylchlorophosphidoborabenzene **2**. As can be seen in Scheme 1, species **2** was obtained from the reaction of 1-chloro-2-(trimethylsilyl)boracyclohexa-2,5-diene (**1**) in presence of one equivalent of $P(tBu)_2Cl$. The reaction works efficiently to generate **2** in a non-reversible manner with the release of Me_3SiCl, as

previously reported by Fu.[18] However the product is not very stable in an isolated dry state and cannot be stored for prolonged periods of time. Monitoring of the reaction by NMR spectroscopy at 333 K allowed the observation of the conversion of **1** to **2** after approximately 6 h. New resonances are observed at 7.98, 7.40, and 7.34 ppm corresponding to the *meta*, *ortho*, and *para* proton positions relative to boron on the borabenzene ring system, respectively. A new resonance for the *tert*-butyl protons also appears at 1.00 ppm (J = 15.8 Hz) while the $^{31}P\{^{1}H\}$ resonance is shifting downfield from 147 ppm for the free phosphine to 121 ppm (q, $^{1}J_{P\text{-}B}$ = 74.5 Hz). The $^{11}B\{^{1}H\}$ resonance is witnessed to shift from 53.5 for **1** to 19.7 for **2** (d, $J_{B\text{-}P}$ = 87.6 Hz).

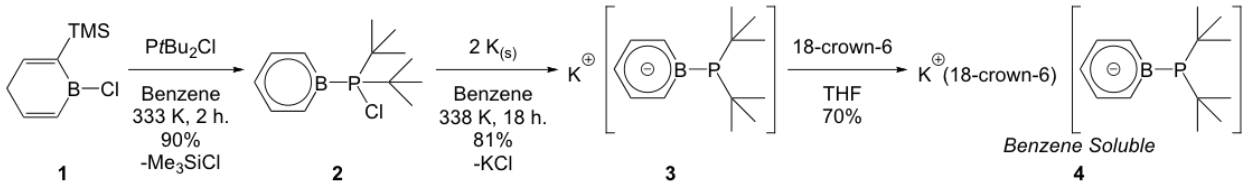

Scheme 1. Synthesis used to generate the $[DTBB]^{-}$ ligand.

Following the synthesis of **2**, reduction was accomplished with liquefied potassium in benzene at 338 K resulting in the formation of the white $K^{+}[DTBB]^{-}$ salt (**3**). The reduced ligand was dissolved in THF and passed through a celite plug, then filtered through an acrodisc before recrystallization from THF by hexane diffusion (81% isolated yield). Monitoring of the reduction progress was accomplished by $^{31}P\{^{1}H\}$ NMR, which revealed near total conversion from **2** to **3** with the formation of a new $^{31}P\{^{1}H\}$ NMR resonance observed at 9.4 ppm (s). Because of the limited solubility of **3**, the 18-crown-6 coordinated compound (**4**) was prepared in order to improve the solubility of the ligand in benzene for subsequent reactivity probing and characterization. The synthetic process for **4** simply required dissolving **3** in THF and adding 18-crown-6 in an amount sufficient to make it the limiting reagent. The THF can then be removed via high vacuum pump

and the product coordinated to 18-crown-6 (**4**) can be extracted with benzene. NMR data for the new compound shows a $^{11}B\{^{1}H\}$ resonance at 34.5 ppm (s), which corresponds nicely to the resonance reported by Fu for $[DPB]^{-}\cdot K^{+}$(18-crown-6) at 31.6 ppm (s).[8a] The $^{31}P\{^{1}H\}$ resonance for **4** is witnessed as a broad singlet at 11.6 ppm.

Single crystals of **3** and **4** were isolated and X-ray data for these species were obtained. The thermal atomic displacement parameter diagrams of both species are observed in Figure 2 and 3, and important bond values are listed within the captions of both respective figures. As can be witnessed in Figure 2B, $K^{+}[DTBB]^{-}$ forms a supramolecular ring composed of six individual $K^{+}[DTBB]^{-}$ ligands. The super-ring structure displays a near perfect hexagonal arrangement with an approximate distance of 11.5 Å between opposing K^{+} centers and a distance of 5.7 Å between adjacent K^{+} centers. The rings are superposed along the c axis but are interconnected by P-B interactions forming an honeycomb structure in the ab plane (Figure 2C). Species **4** crystallizes as a $[DTTB]^{-}\cdot K^{+}$(18-crown-6) species, which allows for direct comparison with the previously published structures for diphenylphosphidoboratabenzene $[DPB]^{-}\cdot K^{+}$(18-crown-6) and diphenylamidoboratabenzene $[DAB]^{-}\cdot K^{+}$(18-crown-6) (as seen in Table 2).[8a] As can be seen in comparing the bond length between the boron and phosphorus atoms in **4** (1.977 Å) with $[DPB]^{-}$ (1.968 Å), a slightly longer bond is witnessed in **4**, which can be attributed to the more sterically bulky *tert*-butyl groups exerting their presence on the boratabenzene system. These bond lengths are however right in the expected range for a single covalent interaction between boron and phosphorus and are dramatically longer than the pronounced overlap within the $[DAB]^{-}$ boron-nitrogen interaction (1.510 Å), which is witnessed to be a much more accurate projection of true double bond character. An overview of the summation of the bond angles around the $[DTBB]^{-}$ and $[DPB]^{-}$ phosphorous centers shows significantly more planarization in **4** than in the $[DPB]^{-}$

species, (319.3° vs. 310.1°, respectively). This is likely caused the steric bulk of the *tert*-Bu groups, but is far from the value of 359.9° witnessed in the $[DAB]^-$ sp^2-hybridized nitrogen center.

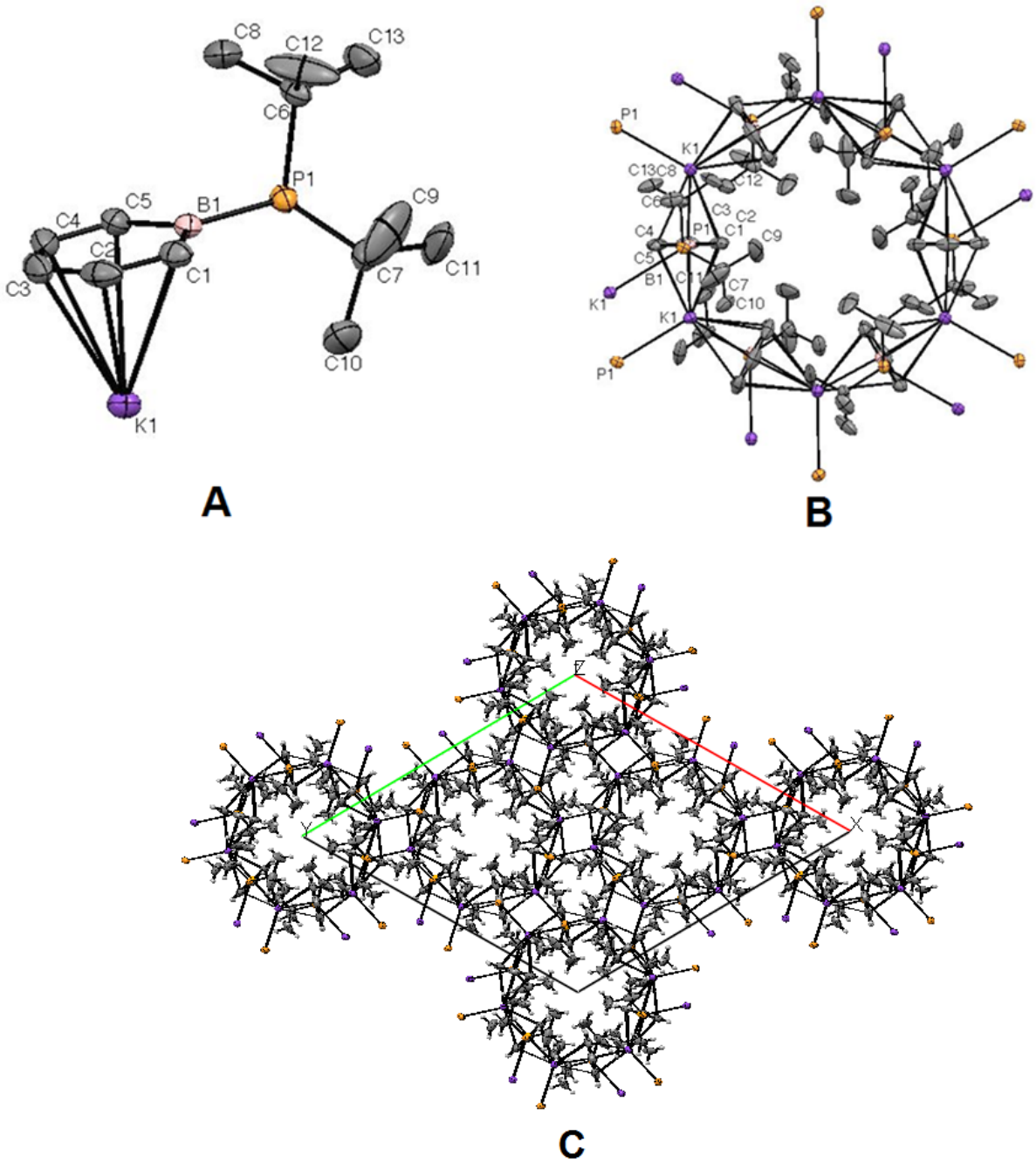

Figure 2. A) Thermal atomic displacement parameter plot of **3,** B) diagram of **3** showing the three coordinate nature of the $[DTBB]^-$ ligand to potassium cations, and C) a packing diagram of **3** with view of the ab plane. Hydrogen atoms have been omitted for clarity. (R_1 = 4.42%) Anisotropic atomic displacement ellipsoids for the non-hydrogen atoms are shown at the 50% probability level. Selected bond distances [Å] and angles [°]: B1-P1 1.965(3), B1-C1 1.503(5), C1-C2 1.401(4), C2-C3 1.389(6), C3-C4 1.389(5), C4-C5 1.394(4), B1-C5 1.509(5), P1-C6 1.904(2), P1-C7 1.900(3), B1-K1 3.317(2), P1-K1 3.371(1), C1-K1 3.249(3), C2-K1 3.142(3), C3-K1 3.096(3), C4-K1 3.140(2), C5-K1 3.232(2), C1-B1-P1 129.9(2), C5-B1-P1 115.8(2), B1-P1-C6 104.3(1), B1-P1-C7 108.6(1), C6-P1-C7 110.0(1).

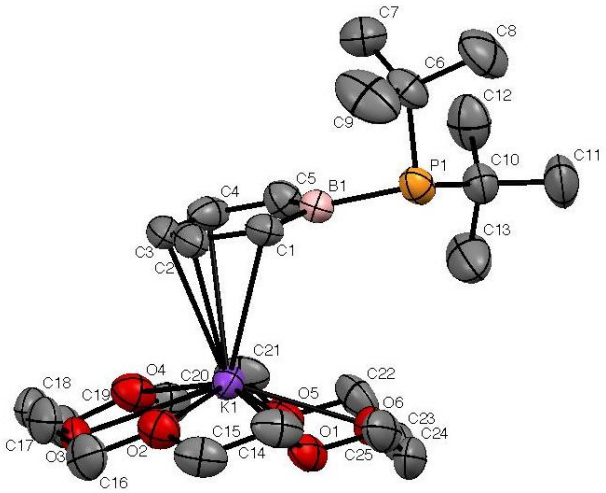

Figure 3. Thermal atomic displacement parameter plot of **4**. Hydrogen atoms have been omitted for clarity. (R_1 = 5.42%) Anisotropic atomic displacement ellipsoids for the non-hydrogen atoms are shown at the 50% probability level. Selected bond distances and angles are in Table 2.

Table 2. Selected bond distances [Å] and angles [°] for **4** relative to $[DPB]^-\cdot K^+$(18-crown-6) and $[DAB]^-\cdot K^+$(18-crown-6)[8a]

$K^+[DTBB]^-$(18-crown-6)		$K^+[DPB]^-$(18-crown-6)		$K^+[DAB]^-$(18-crown-6)	
P_1-B_1	1.977(3)	P_1-B_1	1.968(7)	N_1-B_1	1.510(10)
B_1-P_1-C_6	101.6(1)	B_1-P_1-C_6	102.5(3)	B_1-N_1-C_6	122.7(6)
B_1-P_1-C_{10}	108.7(1)	B_1-P_1-C_{12}	106.2(3)	B_1-N_1-C_{12}	120.2(6)
C_6-P_1-C_{10}	109.0(1)	C_6-P_1-C_{12}	101.4(2)	C_6-N_1-C_{12}	117.0(5)
C_1-B_1-P_1	114.9(2)	C_1-B_1-P_1	117.9(4)	C_1-B_1-N_1	122.9(7)
C_5-B_1-P_1	130.6(2)	C_5-B_1-P_1	126.7(4)	C_5-B_1-N_1	123.8(7)
C_1-B_1-C_5	114.4(3)	C_1-B_1-C_5	115.4(5)	C_1-B_1-C_5	113.2(7)
Angle Summations		**Angle Summations**		**Angle Summations**	
P Center	319.3	P Center	310.1	N Center	359.9
B Center	359.9	B Center	360.0	B Center	359.9

Synthesis of the metal complexes

Although boratabenzene complexes of group 10 transition metals are known, very little research has been performed in the field since the first complexes were reported in the mid 1970`s by Herberich.[5-6,11-13] These reported complexes were variants of traditional π-system bound boratabenzene monomeric complexes of Pt(IV) and Ni(II) synthesized via reactions of boracyclohexadiene species with $[Pt(CH_3)_3I]_4$[11] and $Ni(CO)_4$[12], respectively. A dimeric Ni-Ni bridged species was reported by Herberich as an unstable byproduct from the above specified reaction of a boracyclohexadiene species with $Ni(CO)_4$.[13] Our group has been actively

experimenting with a Pt-Cl-B halide bridged borabenzene species noteworthy as it is the only example of this coordination mode for borabenzene transition metal species ever confirmed.[5,6]

The addition of two equivalents of $K^+[DTBB]^-$ to $NiBr_2(PPh_3)_2$ in THF afforded an immediate shift in color for the reaction crude from the green $NiBr_2(PPh_3)_2$ solution to a reddish-black solution after 6 hours (Scheme 2). For purification of this reaction, the crude mixture was passed through a small alumina column in order to isolate the multiple products discernable by NMR analysis. The main product is a green species eluting off the column first followed immediately by a red species, which upon isolation is observed to slowly convert to the green species over several days. Although attempts were made to discern the character of the ligand-metal interaction for the red fraction, the presence of multiple broad NMR resonances in the aromatic region of the NMR spectrum have yielded little conclusive data for interpretation of the nature of the ligand interaction with the metal species. The isolated green product **5** (Figure 4) witnesses all boratabenzene protons to shift upfield with the *meta*-protons of the boratabenzene ring shifting most dramatically from 7.72 ppm to 6.23 ppm (5.94 ppm *ortho*-protons, 5.47 ppm *para*-protons), indicative of ring coordination to nickel. The $^{31}P\{^1H\}$ NMR resonance of **5** is significantly shifted from the free ligand (9.4 ppm) to -8.9 ppm, while the $^{11}B\{^1H\}$ resonance shifts from -34.5 ppm for the free ligand to -2.1 ppm for the nickel complex.

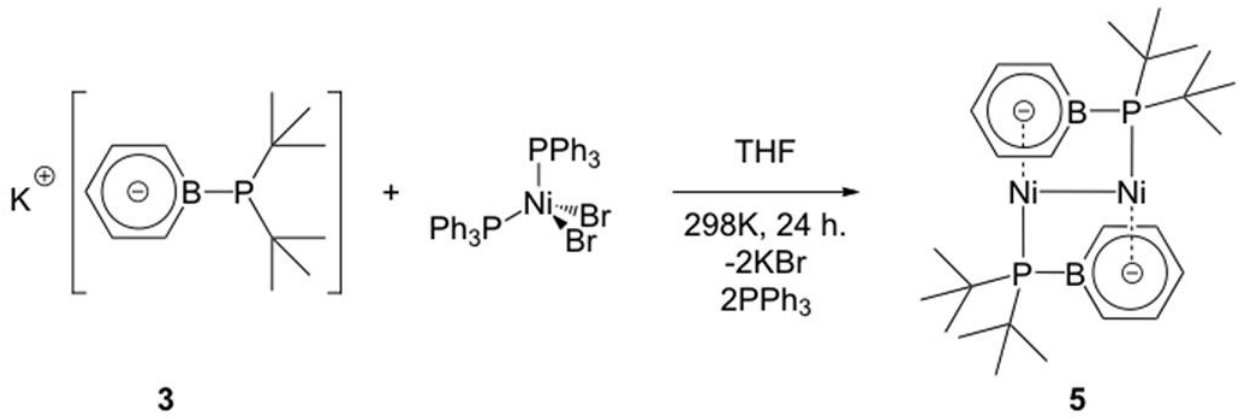

3 5

Scheme 2. Synthetic scheme for the synthesis of the dimeric $Ni_2(DTBB)_2$ species (**5**)

Species **5** crystallizes in the C2/c space group and is disordered over two positions (50:50) where one model is the mirror image of the other. In the unit cell, the P*t*Bu$_2$ moieties are well localized, but the Ni(C_5H_5B) fragment can be tilted over two positions where in one model the phosphorus atom is bound to nickel and where on the other model the phosphorus atom forms a bond with the boron atom (see Supporting Information). The complex **5** consists of an electronically saturated dimer having a Ni-Ni bond length of 2.605(1) Å, which is significantly longer than the 2.30-2.50 Å range expected for these dimers.[14] The phosphidoboratabenzene moiety is bridging the two nickel centers with the η^6-boratabenzene ring coordinated to one metal with all atoms of the heteroaromatic ring more or less equidistant to the nickel (Ni-B/C from 2.113 to 2.279 Å) and with the phosphorous moiety coordinating the other metal (Ni-P of 2.173(7) Å). The phosphorus atom is significantly out of the plane of the boratabenzene ring, with a tilt angle of 22°.

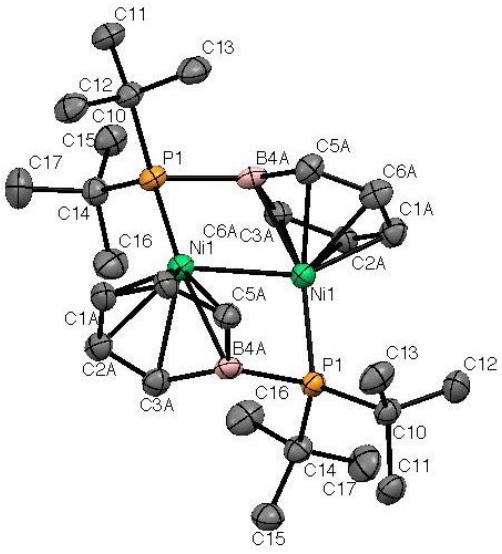

Figure 4. Thermal atomic displacement parameter plot of **5**. Hydrogen atoms have been omitted for clarity. (R_1 = 3.35%) Anisotropic atomic displacement ellipsoids for the non-hydrogen atoms are shown at the 50% probability level. Selected bond distances [Å] and angles [°]: Ni1-P1 2.173(7), Ni1-B4 2.222(5), Ni1-C3 2.279(4), Ni1-C2 2.240(4), Ni1-C1 2.132(4), Ni1-C6 2.134(4), Ni1-C5 2.113(4), Ni1-Ni1 2.605(1), B4-P1 1.990(5), B4-C3 1.534(7), C3-C2 1.388(8), C2-C1 1.418(7), C1-C6 1.411(6), C6-C5 1.394(7), B4-C5 1.547(6), Ni1-Ni1-P1 92.9(3), Ni1-Ni1-B4 70.1(1), B4-Ni1-P1 158.3(1), P1-B4-Ni1 111.1(2), B4-P1-Ni1 84.0(1), C10-P1-Ni1 118.3(6), C14-P1-Ni1 118.1(6), C10-P1-C14 111.1(8).

When $PtCl_2$ was reacted with two equivalents of $[DTBB]^-$, the bis-phosphine complex **6** was formed (Scheme 3). As in complex **5** the boratabenzene *ortho* and *para*-protons are all witnessed to shift upfield when coordinated to the Pt(II) center (6.65 and 6.86 ppm respectively); however, in this case the *meta*-protons are observed to shift downfield from 7.72 to 7.78 ppm. The $^2J_{Pt\text{-}H}$ couplings for the *para* and *ortho* boratabenzene protons are of 21.6 Hz and 47.6 Hz, respectively, but no resolved coupling is observed for the *meta* position. The *tert*-butyl protons are now witnessed to appear as a virtual triplet centered at 1.19 ppm (t, J = 7.5 Hz, 36H) as opposed

to a doublet in the free ligand. $^{11}B\{^{1}H\}$ and $^{31}P\{^{1}H\}$ NMR resonances for **6** are observed as broad singlets appearing at 10.0 ppm and 31.9 ppm, respectively. Also present in the $^{31}P\{^{1}H\}$ NMR spectra are prominent resonances corresponding to ^{195}Pt coupling observed at 31.8 ppm (d, $J_{Pt\text{-}P}$ = 1745 Hz). Coordination of the ligand was observed under variable temperature NMR conditions (Figure 5). As can be seen by the ^{1}H NMR data, coalescence occurs at 200 K and at 186 K new borabenzene resonances appear at altered locations relative to their positions at room temperature (7.91, 7.63, 7.14, 6.88, and 5.86 ppm) and integrate for 5 protons. The notable feature is that the *ortho* proton at 5.86 ppm has a $^{2}J_{Pt\text{-}H}$ of 95.1 Hz, which is twice that of the *ortho* protons at room temperature. The later result indicates that the $[R_2P\text{-}BR{=}CR_2]^-$ moiety of the phosphidoboratabenzene ligand rapidly migrates to have either of the *ortho* carbon coordinated on the metal center and only the average $^{2}J_{Pt\text{-}H}$ is observed at room temperature.

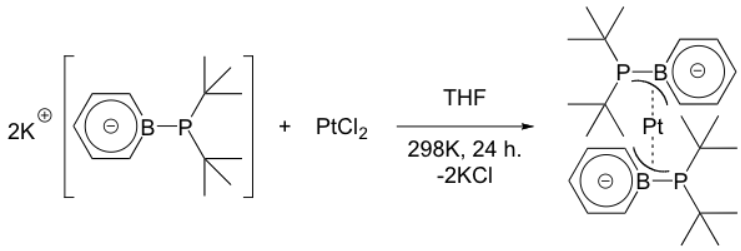

3 **6**

Scheme 3. Reaction yielding the bis-phosphine $Pt(DTBB)_2$ (**6**) species shown below

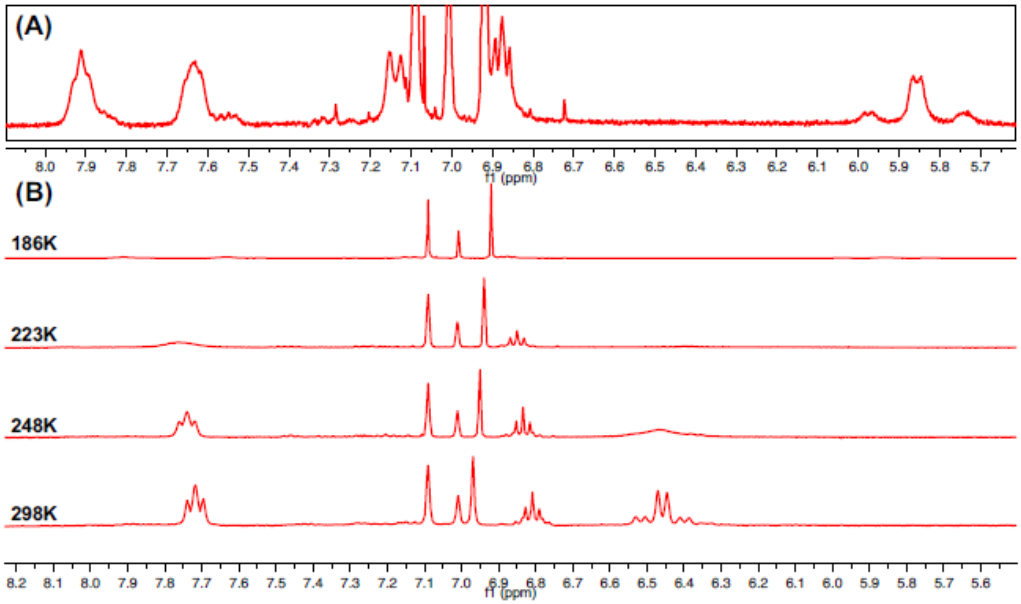

Figure 5. (A) Intensified VT-NMR data for Pt(DTBB)$_2$ **6** in toluene-d$_8$ at 186K. **(B)** Selected spectra from the VT-NMR experiments done at a wide range of temperatures.

Isolation of single crystals of **6** allowed for structure determination, as shown in Figure 6. This new species is seen to exhibit η^3-coordination of both [DTBB]$^-$ ligands in an allyl-like fashion common in recent reported literature by Stephan[15] and by Emslie.[16] One interesting point to note is the significant planarization of the phosphorus center in the species indicated by examination of the bond angles (bond angle summation for phosphorus in species **6** is 344.9° versus a phosphorus angle summation of 333.1° for species **5**). These values can both be contrasted against species **3** which displays an angle summation of 322.9° for phosphorus to show the dramatic planarization of the phosphorus center when coordinated to a metal. A break in the aromaticity of the boratabenzene ring is observed and the double bonds are localized, as can be observed by the short C10-C11 and C12-C13 distances (1.359(6) and 1.367(6) Å, respectively) compared to the C9-C10 and C11-C12 distances (1.443(5) and 1.423(6), respectively). However, there is no significant difference in the B1-C9 and B1-C13 distances (1.527(5) and 1.529(5) Å, respectively) even if a

shorter bond is expected on the account the localization of the double bond in the aromatic ring. In addition, the B1-P2 bond length in **6** is significantly shorter (1.912(4) Å), than what was observed in species **3**-**5** (1.977 to 1.990 Å). This indicates that the coordination is much more akin to an allylic interaction, with a fragment $[R_2P\text{-}BR{=}CR_2]^-$ having an anionic charge delocalized only over the three atoms interacting with the platinum center.

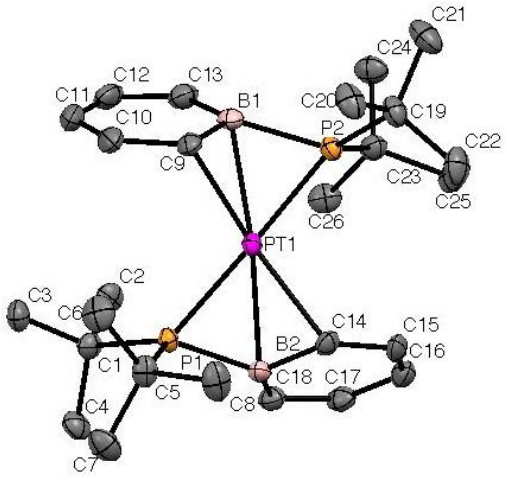

Figure 6. Thermal atomic displacement parameter plot of **6.** Hydrogen atoms have been omitted for clarity. (R_1 = 2.84%) Anisotropic atomic displacement ellipsoids for the non-hydrogen atoms are shown at the 50% probability level. Selected bond distances [Å] and angles [°]: Pt1-P1 2.327(1), Pt1-B1 2.379(4), Pt1-C9 2.268(3), Pt1-P2 2.329(8), Pt1-B2 2.370(4), Pt1-C14 2.276(3), B1-P2 1.907(4), B2-P1 1.912(4), P1-Pt1-P2 172.5(3), P1-Pt1-B1 129.6(10), P1-Pt1-C9 103.7(9), B2-Pt1-P2 130.2(10), B2-Pt1-B1 154.1(13), B2-Pt1-C9 151.7(13), C14-Pt1-P2 104.3(9), C14-Pt1-B1 152.0(13), C14-Pt1-C9 154.9(13), C19-P2-C23 112.4(16), C19-P2-B1 118.6(17), C23-P2-B1 113.9(17), C1-P1-C5 113.2(15), C1-P1-B2 113.3(16), C5-P1-B2 118.7(16).

Reported literature results for this type of boratabenzene interaction with a transition metal show this type of three coordinate "allyl" interaction with a metal center within a scandium complex.[17] The reported dimeric scandium complex is observed through crystallographic characterization to coordinate to a dimethylamidoboratabenzene species in a planar allylic manner closely akin to the coordination mode of platinum. However, the scandium adduct coordinates to a nitrogen exocyclic ring adduct, not a phosphorus adduct as observed in $Pt(DTBB)_2$ **6**. The distances for the interaction are reported as 2.316 Å (Sc-N), 2.569 Å (Sc-B), and 2.457 Å (Sc-C). The value for the Sc-N interaction (2.316 Å) is remarkably close to the reported value for the Pt-P interaction in $Pt(DTBB)_2$ (2.327 Å), but the subsequent distances for Sc-B and Sc-C interactions display a planar ligand coordinated at an angle away from the metal center while the bond distances for Pt-B (2.379 Å) and Pt-C (2.268 Å) indicate that $[DTBB]^-$ binds more equidistant to the metal center. These data indicate that the overlap between the phosphidoboratabenzene and the platinum(II) core is more efficient than in the scandium complex, even if the atomic radii of scandium is significantly smaller than that of platinum. DFT calculations have been carried out on species **6** to gain more details on the nature of this "allylic" interaction. As can be observed in Figure 7, the electron delocalization over the $[R_2P\text{-}BR{=}CR_2]^-$ fragment is important and is typical of the HOMO-1 of an allylic ligand (fully delocalized over the three centers). Moreover, the three interactions with the platinum center are quite clear as demonstrated by the Wiberg indices of 0.69, 0.29 and 0.33 for the Pt-P, Pt-C and Pt-B, respectively. Although the Pt-P and Pt-C interactions were found at the first order NBO analysis, confirming a bonding interaction, the Pt-B one was found at the NBO second order level (20 $kcal.mol^{-1}$), meaning that it is rather a donor-acceptor interaction than a real bond. The Wiberg indexes for the P-B and P-C bonds are respectively 1.0755

and 1.1025, indicative that the bonding is more than a classical single bond and that electron density is shared between the three atoms.

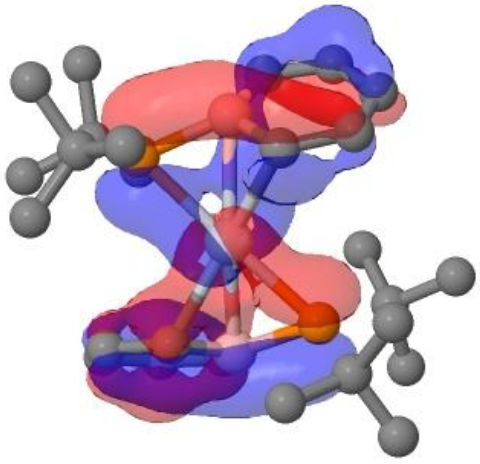

Figure 7. Representation of the HOMO-2 in complex **6**.

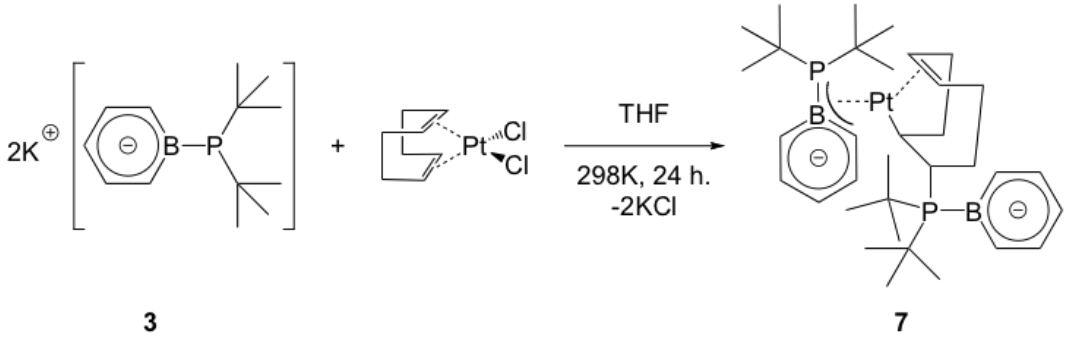

3 **7**

Scheme 4. Reaction scheme used to synthesize (η^3-(C,B,P)-$C_5H_5BP(t\text{Bu})_2$)(κ-η^2:η^1-$C_8H_{12}(P(t\text{Bu})_2BC_5H_5)Pt$ (**7**)

Coordination studies of $[DTBB]^-$ with $PtCl_2COD$ were also carried out as can be seen in Scheme 4. Although the reaction mixture proved to be quite complex, a few crystals were eventually isolated, which proved sufficient for NMR characterization and to allow for the elucidation of the connectivity using X-ray diffraction (Figure 8). Species **7** consists of a platinum(II) species where the $[DTBB]^-$ is bound in an allylic fashion as observed in **6**, but with a κ-η^2:η^1-3-cycloocten-1-yl fragment originating from the attack by the phosphorous moiety of the $[DTBB]^-$ anion on the coordinated 1,5-cyclooctadiene in $PtCl_2COD$. NMR data for complex **7** showcased two sets of resonances in the $^{31}P\{^1H\}$ spectrum at 41.2 and 37.2 ppm effectively corresponding to the two different phosphorus environments in the species. The resonance at 37.2 is also witnessed to display prominent ^{195}Pt satellites with a coupling constant of 2920 Hz. The $^{11}B\{^1H\}$ spectrum for this complex displays two prominent resonances for the respective boron environments at 18.8 and 9.4 ppm respectively. However, due to the low concentration of the sample no ^{195}Pt coupling could be discerned. This data is relatively close to the reported $^{11}B\{^1H\}$ boron shift for the (1,3,4-η^3-3-cycloocten-1-yl)(1-phenylborinato)nickel complex prepared by Herberich, which displays a chemical shift of 22.4 ppm.[12] In the X-ray structure, a first $[DTBB]^-$ is bound in an allylic fashion with bond lengths close to that observed in **6**, considering the large deviation caused by the poor quality of the crystal. The Pt-P, Pt-B and Pt-C distances of the $[R_2P\text{-}BR{=}CR_2]^-$ fragment in **7** are of 2.28(4), 2.40(2), and 2.38(1) Å respectively, compared to values of 2.327(1), 2.379(4), and 2.268(3) Å observed for the respective Pt-P, Pt-B and Pt-C bond lengths in **6**. The longer Pt-C bond in **7** when compared to the values found in **6** could be attributed to the larger *trans* influence of the alkyl group (C13) *trans* to C4 in **7** than of the boraalkene fragment in **6**.

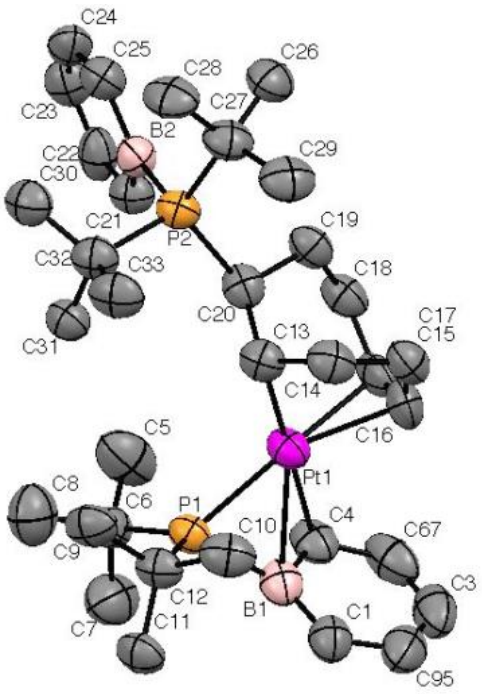

Figure 8. Thermal atomic displacement parameter plot of **7.** Hydrogen atoms have been omitted for clarity. (R_1 = 8.18%) Anisotropic atomic displacement ellipsoids for the non-hydrogen atoms are shown at the 50% probability level. Selected bond distances [Å] and angles [°]: Pt1-P1 2.28(3), Pt1-B1 2.40(2), Pt1-C4 2.38(1), Pt1-C13 2.08(1), Pt1-C16 2.18(1), Pt1-C17 2.20(1), B1-P1 1.93(2), B1-C4 1.49(2), P2-C20 1.89(1), P2-B2 1.93(2), C6-P1-Pt1 117.8(5), C12-P1-Pt1 119.0(4), B1-P1-Pt1 68.8(5).

Conclusion

Although it was reported by Fu that the phosphidoboratabenzene moiety serves as an anionic analogue of the ubiquitous phosphine ligands,[7] we have shown that the coordination of the π system of the boratabenzene moiety to an unsaturated metal center is a viable alternative to phosphine coordination. The DFT models are in accordance with this observation since the HOMO

is mainly centered on the ring system. In order to demonstrate such behavior, the di-*tert*-butylphosphidoboratabenzene $[DTBB]^-$ ligand has been successfully synthesized and coordinated within the framework of three different group 10 metal complexes. The new species have all been characterized and their structures elucidated by X-ray crystallography. In the case of the nickel complex, the $[DTBB]^-$ serves as a bridging ligand for the formation of a dimeric Ni(I) species having a relatively long Ni-Ni bond. The $[DTBB]^-$ bridges the nickel center by coordination of the boratabenzene ring in a η^6 fashion to one metal and by phosphine coordination to the other. In the two structurally characterized platinum(II) complexes, the $[R_2P\text{-}BR{=}CR_2]^-$ fragment is shown to prefer coordination in a η^3 manner similar to the boratapropargyl and borataallyl species recently reported and discussed by Stephan[15] and Emslie.[16] In the continuation of this work, we are currently looking at the reactivity of these complexes and also at ways to prevent the interaction of the π system of phosphidoboratabenzene analogues to unsaturated metal centers.

Experimental Section

General Methods

All operations were carried out under an atmosphere of nitrogen using standard Schlenk techniques or in nitrogen filled gloveboxes. Benzene, THF, and pentane were all distilled from Na-benzophenone ketyl. Deuterated solvents (C_6D_6 and toluene-d_8) were dried over sodium-potassium amalgam and collected via distillation. 1-Chloro-2-(trimethylsilyl)boracyclohexa-2,5-diene was prepared according to the procedure described by Fu.[18a] Di-tert-butylchlorophosphine and 18-crown-6 were purchased from Sigma-Aldrich. Bis(triphenylphosphine)nickel(II) bromide and platinum(II) chloride were purchased from Alfa Aesar. Dichloro(1,5-

cyclooctadiene)platinum(II) was prepared according to the methods outlined in Inorganic Synthesis.[19] ^{1}H, ^{13}C and ^{31}P NMR spectra were recorded on either a Bruker NMR AC-300 spectrometer or a Varian Inova NMR AS400 spectrometer at 300 and 400 MHz, 75 and 100 MHz, or 121 and 161 MHz respectively. ^{11}B NMR spectra were recorded on the Varian Inova NMR AS400 spectrometer at 128 MHz. The temperature during VT NMR was calibrated using the difference in chemical shift between the two resonances of methanol. All chemical shifts were reported in δ units with reference to the residual solvent resonance of the deuterated solvents for proton and carbon chemical shifts. Elemental analysis was performed by Midwest Microlab, LLC (Indianapolis, IN, USA). HRMS characterization was possible using an Agilent Technologies 6210 LC Time of Flight Mass Spectrometer. Products in toluene solutions were introduced to the nebulizer by direct injection. Neutral borabenzene adducts were characterized using APPI ionization in positive mode. Ionic species were ionized by electrospray (ESI-MS) in both positive and negative modes

Di-*tert*-butychlorophosphidoborabenzene (2)

Di-*tert*-butylchlorophosphine (2.092 g, 11.58 mmol) was added dropwise to a solution of 1-chloro-2-(trimethylsilyl)boracyclohexa-2,5-diene (2.176 g, 11.79 mmol) in 25 mL of benzene at 298K. The reaction mixture was heated to 338K and allowed to react over 2.5 h. The solvent and TMSCl byproduct were removed via vacuum followed by addition of fresh benzene and subsequent solvent removal via vacuum. It is imperative to remove as much TMSCl as possible. The compound is not stable in the solid state and must be used immediately in the subsequent reductions step. The product is unstable in the solid state (off-white solid).

^{1}H NMR [300 MHz] (C_6D_6) δ: 7.98 (br q, J_{H-H} = 7.8 Hz, 2H), 7.39 (m, 3H), 1.00 (d, J_{H-P} = 15.8 Hz, 18H). ^{13}C NMR [75 MHz] (C_6D_6) δ: 133.8 (s), 133.5 (s) 121.1 (br s), 38.3 (d, J_{C-P} = 15.4 Hz), 27.2 (d, J_{C-P} = 4.1 Hz). ^{11}B{^{1}H} NMR [128 MHz] (C_6D_6) δ: 19.7 (d, J_{P-B} = 87.6 Hz). ^{31}P{^{1}H} NMR [121 MHz] (C_6D_6) δ: 120.7 (q, J_{P-B} = 74.5 Hz).

Potassium Di-*tert*-butylphosphidoboratabenzene (3)

Di-*tert*-butylchlorophosphidoboratabenzene (2.97 g, 11.6 mmol) was dissolved in 25 mL of benzene and reduced by canulation of the solution into a degassed Schlenk containing (1.10 g, 28.1 mmol) $K_{(s)}$. The mixture was heated to just below benzene reflux (338K) and allowed to reduce for 18 h. Workup of the compound was undertaken by solvent removal *in vacuo* and extraction via THF washings. Collection of crystalline product was undertaken by filtration and recrystallization of this THF extraction. Yield: 81% (2.45 g, 9.42 mmol) of an off-white powder.

^{1}H NMR [400 MHz] (THF-d^8) δ: 7.27 (m, 2H), 6.93 (m, 2H), 6.31 (ttd, J_{H-H} and J_{H-P} = 6.9, 1.3, 0.7 Hz, 1H), 1.33 (d, J_{H-P} = 10.0 Hz, 18H). ^{13}C NMR [101 MHz] (THF-d^8) δ: 134.8 (br s), 132.5 (d, J_{C-P} = 10.1 Hz), 112.7 (br s), 69.7 (s), 33.7 (d, J_{C-P} = 12.4 Hz), 30.8 (d, J_{C-P} = 23.7 Hz). ^{11}B{^{1}H} NMR [128 MHz] (THF-d^8) δ: 17.3 (br d, J_{B-P} = 79.5 Hz). ^{31}P{^{1}H} NMR [121 MHz] (C_6D_6) δ: 7.84 (br s). Anal. Calcd. for $C_{13}H_{23}BPK$: C, 60.01; H, 8.91. Found: C, 59.09; H, 8.60.

K^+[DTBB]$^-$(18-crown-6) (4)

18-crown-6 (0.0071 g, 0.027 mmol) was dissolved in 3 mL of THF and added into a 1 dram vial containing K^+[DTBB]$^-$ (0.0071 g, 0.027 mmol). The reactants were vigorously agitated until all reagents were observed to be dissolved. The THF solution was filtered via acrodisc into a small Schlenk flask. Solvent removal was conducted under vacuum and the product was collected as a white powder. Yield: 70% (0.0098 g, 0.019 mmol) of a white powder.

^{1}H NMR [400 MHz] (C_6D_6) δ: 7.72 (ddd, J_{H-H} = 7.4, 6.8, 3.5 Hz, 2H), 7.42 (ddd, J_{H-H} = 10.2, 3.7, 1.2 Hz, 2H), 6.65 (t, J_{H-H} = 6.9 Hz, 1H), 3.09 (br s, 24H), 1.82 (d, J_{H-P} = 9.8 Hz, 18H). ^{13}C NMR [101 MHz] (C_6D_6) δ: 132.5 (br s), 132.2 (d, J_{C-P} = 9.1 Hz), 111.4 (br s), 69.7 (s), 33.8 (d, J_{C-P} = 12.1 Hz), 31.3 (d, J_{C-P} = 21.5 Hz). ^{11}B{^{1}H} NMR [128 MHz] (C_6D_6) δ: 34.5 (br s). ^{31}P{^{1}H} NMR [121 MHz] (C_6D_6) δ: 11.6 (br s).

$Ni_2(DTBB)_2$ (5)

$K^+[DTBB]^-$ (0.233 g, 0.894 mmol) was dissolved in 5 mL of THF and added to a small Schlenk flask containing $NiBr_2(PPh_3)_2$ (0.298 g, 0.401 mmol) and a stirbar. This reaction was stirred for a period of 24 h. The reaction mixture was purified by solvent removal and the product was extracted with 10 mL of benzene. A primary filtration procedure was undertaken by passing the extracted benzene layer through a filter disk placed within a pipette before final filtration through an acrodisk. Alumina column purification (pentane as eluent) of crude yielded emerald green product. Yield: 25% (0.0556 g, 0.0998 mmol) of an emerald-green solid.

^{1}H NMR [400 MHz] (C_6D_6) δ: 6.23 (m, 4H), 5.94 (m, 4H), 5.47 (tt, J_{H-H} = 6.1, 1.2 Hz, 2H), 1.38 (d, J_{H-P} = 13.0 Hz, 36H). ^{13}C NMR [101 MHz] (C_6D_6) δ: 112.1 (d, J_{C-P} = 8.4 Hz), 110.1 (br s), 83.1 (s), 33.1 (d, J_{C-P} = 16.1 Hz) 33.1 (s). ^{11}B{^{1}H} NMR [128 MHz] (C_6D_6) δ: -2.2 (br s). ^{31}P{^{1}H} NMR [121 MHz] (C_6D_6) δ: -8.9 (br s). DI-MSTOF (APPI, *m/e*) calcd for $C_{26}H_{46}B_2P_2Ni_2$ 556.204; found 556.2057.

$Pt(DTBB)_2$ (6)

$K^+[DTBB]^-$ (0.050 g, 0.19 mmol) was dissolved in 5 mL of THF and added to a 20 mL vial containing $PtCl_2$ (0.021 g, 0.079 mmol) and a stirbar. This reaction was stirred for a period of 48 h. The reaction mixture was purified by solvent removal and the product extracted with 10 mL of

pentane. Alumina column purification (pentane as eluent) of crude yielded one fraction (canary yellow). Yield: 26% (0.013 g, 0.020 mmol) of a yellow solid.

^{1}H NMR [400 MHz] (C_6D_6) δ: 7.78 (t, $J_{H\text{-}H}$ = 8.8 Hz, 4H), 6.86 (t, $J_{H\text{-}H}$ = 7.4 Hz with $J_{H\text{-}Pt}$ = 21.6 Hz, 2H), 6.53 (d, $J_{H\text{-}H}$ = 9.9 Hz with $J_{H\text{-}Pt}$ = 47.6 Hz, 4H), 1.19 (t, $J_{H\text{-}P}$ = 7.5 Hz, 36H). ^{13}C NMR [101 MHz] (C_6D_6) δ: 141.4 (t, $J_{C\text{-}P}$ = 6.0 Hz), 123.4 (s with $J_{C\text{-}Pt}$ = 25.0 Hz), 109.2 (br s), 33.4 (s with $J_{C\text{-}Pt}$ = 23.2 Hz), 31.7 (t, $J_{C\text{-}P}$ = 2.2 Hz with $J_{C\text{-}Pt}$ = 15.0 Hz). ^{11}B{^{1}H} NMR [128 MHz] (C_6D_6) δ: 10.0 (br s). ^{31}P{^{1}H} NMR [121 MHz] (C_6D_6) δ: 31.9 (s) 31.8 (d, $J_{P\text{-}Pt}$ = 1745 Hz). DI-MSTOF (APPI, *m/e*) calcd for $C_{26}H_{46}B_2P_2Pt$ 630.2933; found 630.2925.

Pt(DTBB)$_2$(COD) (7)

$K^{+}[DTBB]^{-}$ (0.051 g, 0.20 mmol) was dissolved in 5 mL of THF and added to a 20 mL vial containing $PtCl_2COD$ (0.032 g, 0.086 mmol) and a stirbar. This reaction was stirred for a period of 96 h within a small glovebox. The product and solvent were then transferred to a small Schlenk flask equipped with a stirbar. The solvent was then removed under oil vacuum pump and the product was extracted with benzene (yellow solution). The liquid was then passed through an acrodisc 0.2 μm filter followed by solvent removal and product collection (yellow solid). Yield: some crystals of X-ray quality.

^{1}H NMR [400 Mz] (C_6D_6) δ: 8.04 (ddd, $J_{H\text{-}H}$ = 10.6, 7.2, 4.8 Hz, 2H), 7.67 (ddd, $J_{H\text{-}H}$ = 10.5, 7.3, 3.5 Hz, 2H), 7.29 (m, 5H), 6.72 (dd, $J_{H\text{-}H}$ = 10.2, 3.7 Hz, 1H), 4.90 (d, $J_{H\text{-}H}$ = 8.4 Hz 1H), 4.54 (d, $J_{H\text{-}H}$ = 7.8 Hz, 1H), 4.22 (dt, $J_{H\text{-}H}$ = 10.6, 5.5 Hz 2H), 2.11 (m, 8H), 1.38 (m, 36H). ^{11}B{^{1}H} NMR [128 MHz] (C_6D_6) δ: 18.8 (br s), 9.4 (br s). ^{31}P{^{1}H} NMR [121 MHz] (C_6D_6; referenced to H_3PO_4) δ: 41.2 (very br s), 37.2 (s), 37.2 (d, $J_{P\text{-}Pt}$ = 2918 Hz).

Structural studies

Crystalline samples of compounds **3**, **4**, and **7** were grown by slow evaporation of solvated pure samples of material contained within glass vessels. Crystalline samples of compounds **5** and **6** were grown by slow evaporation of solvated chromatographed fractions within small Teflon Eppendorf containers. X-ray data for compound **3** were collected at 110 K on a Bruker APEX II dual source diffractometer using the Incoatec Microfocus IMuS source with copper CuKα radiation (1.54178 Å). For compounds **5**, **6** and **7**, the measurements were performed at 150 K on a Bruker Microstar area detector diffractometer equipped with a rotating anode generator also producing CuKα radiation. Data for compound **4** were collected at 200 K on a Bruker APEX II diffractometer equipped with graphite monochromated MoKα radiation. The program used for retrieving cell parameters and data collection was APEX 2,[20] the data were integrated using the program SAINT[21] and were corrected for Lorentz and polarization effects. The multiscan absorption corrections were performed using SADABS.[22] The structures were solved and refined using SHELXS-97 and SHELXL-97 (Sheldrick, 1997)[23] and all non-H atoms were refined anisotropically, with the hydrogen atoms placed at idealized positions. The crystallographic data are given in Table 3.

Table 3. Pertinent information concerning the collection and treatment of X-ray diffraction data collected for all structures published within this report.

	3	**4**	**5**	**6**	**7**
formula	$C_{13}H_{23}BKP$	$C_{25}H_{47}BKO_6P$	$C_{26}H_{46}B_2Ni_2P_2$	$C_{26}H_{46}B_2P_2Pt$	$C_{37}H_{60}B_2P_2Pt$
fw	260.19	524.51	559.61	637.28	783.5
temp	110(2) K	200(2)	150(2)	150(2)	150(2)
λ, Å	1.54178	0.71073	1.54178	1.54178	1.54178
system	trigonal	monoclinic	monoclinic	triclinic	triclinic
space group	R-3	P2(1)/c	C2/c	P-1	P-1
a, Å	23.8882(3)	14.692(3)	21.8531(7)	9.3833(3)	8.6500(17)
b, Å	23.8882(3)	22.825(4)	14.5902(5)	10.6385(4)	11.990(2)
c, Å	14.1077(3)	9.1192(18)	9.0390(3)	21.9552(8)	18.210(4)
α, deg	90	90	90	77.0532(14)	106.09(3)
β, deg	90	100.168(2)	107.2040(10)	83.1099(13)	94.29(3)
γ, deg	120	90	90	77.0269(12)	103.88(3)
U, Å^3	6971.94(19)	3010.0(10)	2753.06(16)	2075.82(13)	1741.3(6)
Z	18	4	4	3	2
d_{calc}, Mg/m^3	1.115	1.157	1.35	1.529	1.494
abs coefficient, mm^{-1}	3.745	0.263	2.867	10.638	8.569
F(000)	2520	1136	1192	960	800
crystal dimens, mm	0.33x0.24x0.12	0.17x0.17x0.03	0.22x0.18x0.10	0.08x0.08x0.06	0.15x0.12x0.08
θ range for data collection	3.70 to 65.98	1.41 to 26.00	3.70 to 69.34	2.07 to 69.98	2.55 to 67.50
abs corr	semi-empirical from equivalents	integration	integration	semi-empirical from equivalents	integration
no. of reflns	7348	32183	25918	30464	71065
no. of indep obs reflns	2407	3556	2535	5150	5150
I > 2σ(I)					
R(int)	0.0281	0.0806	0.0414	0.043	0.0868
R1	0.0442	0.0542	0.0335	0.0284	0.0818
R2	0.1081	0.1151	0.0891	0.0747	0.2117
GOF on F^2	1.038	1.016	1.144	1.042	1.183

Computational studies

All the calculations were performed with the Gaussian 03 suite of programs.[24] The density functional theory calculations for the $[DPB]^-$, the $[DTBB]^-$ and the nickel complexes were carried out as previously described by Gusev for evaluation of the electron donating property of a series of two electron donor ligands.[10] The MPW1PW91[25] hybrid functional was employed. The 6-

311+g(2D) basis set was used for Ni and 6-311+g(p,d) for all other atoms.[26] Tight geometry optimizations were performed with an ultrafine integration grid, without symmetry constraints.[27] Vibrational analyses were performed to confirm the optimized stationary points as true minima on the potential energy surface and to obtain the zero-point energy, thermodynamic data and stretching frequencies. Molecular orbital representations were drawn with an isovalue of 0.02.

For the model of species **6**, the platinum and the phosphorus were treated with a Stuttgart-Dresden pseudopotential in combination with their adapted basis set.[28] The basis set has been augmented by a set of f polarization functions[29] to the platinum and by a set of d polarization functions to phosphorus atoms. Carbon, boron and hydrogen atoms have been described with a 6-31G(d,p) double-ζ basis set.[30] Calculations were carried out at the density functional theory (DFT) level of theory using the hybrid functional B3PW91.[31] Geometry optimizations were carried out without any symmetry restrictions and the nature of the extremum (minimum) was verified with analytical frequency calculations. The calculations were carried out in the gas phase. The electron density has been analyzed using the Natural Bonding Analysis (NBO).[32]

Supporting Information Available: NMR characterization for compounds **2-7**. Cartesian coordinates and energy for compounds **[DPB]**$^{-}$, **[DTBB]**$^{-}$**, [DPB]**$^{-}$**Ni(CO)**$_3$**, [DTBB]**$^{-}$**Ni(CO)**$_3$**,** and **6.** Crystallographic data have been deposited with CCDC (CCDC No. 891933 for **3**, CCDC No. 891934 for **4**, CCDC No. 891935 for **5**, CCDC No. 891936 for **6**, and CCDC No. 891937 for **7**). These data can be obtained upon request from the Cambridge Crystallographic Data Centre, 12 Union Road, Cambridge CB2 1EZ, UK, e-mail: deposit@ccdc.cam.ac.uk, or via the internet at www.ccdc.cam.ac.uk.

Acknowledgment. We are grateful to NSERC (Canada), CFI (Canada), FQRNT, CCVC (Québec), and CERPIC (Université Laval) for financial support. J.B. is grateful to NSERC, FQRNT, and Rio-Tinto Alcan for scholarships. Calmip and CINES are acknowledged for generous grant of computing time. LM is member of the Institut Universitaire de France

References

[1] (a) Fu, G. C. *Adv. Organomet. Chem.* **2001**, *47*, 101–119. (b) Herberich G. E.; Ohst, H. *Adv. Organomet. Chem.* **1986,** *25*, 199–236. (c) Ashe, A. J. III; Al-Ahmad S.; Fang, X. *J. Organomet. Chem.* **1999**, *581*, 92-97.

[2] (a) Bönnemann, von H.; Brijoux, W.; Brinkmann R.; Meurers, W. *Helv. Chem. Acta* **1984**, *67*, 1616-1624. (b) Bazan, G. C.; Rodriguez, G.; Ashe, A. J. III; Al-Ahmad S.; Kampf, J. W. *Organometallics* **1997**, *16*, 2492-2494. (c) Ashe, A. J. III; Al-Ahmad, S.; Fang X.; Kampf, J. W. *Organometallics* **1998**, *17*, 3883-3888. (d) Rogers, J. S.; Bu X.; Bazan, G. C. *Organometallics* **2000**, *19*, 3948-3956. (e) Komon, Z. J. A.; Rogers, J. S.; Bazan, G. C. *Organometallics* **2002**, *21*, 3189-3195. (f) Cui, P.; Chen, Y.; Zeng, X.; Sun, J.; Li, G. Xia, W. *Organometallics* **2007**, *26*, 6519-6521. (g) Rogers, J. S.; Bu, X.; Bazan, G. C. *J. Am. Chem. Soc.* **2000**, *122*, 730-731. (h) Rogers, J. S.; Bazan, G. C.; Sperry, C. K. *J. Am. Chem. Soc.* **1997**, *119*, 9305-9306. (i) Woodmansee, D. H.; Bu, X.; Bazan, G. C. *Chem. Commun.* **2001**, 619-620.

[3] (a) Lee, B. Y.; Wang, S.; Putzer, M.; Bartholomew, G. P.; Bu, X.; Bazan, G. C. *J. Am. Chem. Soc.* **2000**, *122*, 3969-3970. (b) Behrens, U.; Meyer-Friedrichsen, T.; Heck, J. *Z. Anorg. Allg. Chem.* **2003**, *629*, 1421-1430. (c) Jaska, C. A.; Emslie, D. J. H.; Bosdet, M. J. D.; Piers, W. E.;

Sorensen, T. S.; Parvez, M. *J. Am. Chem. Soc.* **2006**, *128*, 10885-10896. (d) Wood, T. K.; Piers, W. E.; Keay, B. A.; M. Parvez, M. *Angew. Chem., Int. Ed.* **2009**, *48*, 4009-4012. (e) Wood, T. K.; Piers, W. E.; Keay, B. A.; Parvez, M. *Chem. Eur. J.* **2010**, *16*, 12199-12206. (f) Hagenau, U.; Heck, J.; Hendrickx, E.; Persoons, A.; Schuld, T.; Wong, H. *Inorg. Chem.* **1996**, *35*, 7863-7866. (g) Emslie, D. J. H.; Piers, W. E.; Parvez, M. *Angew. Chem. Int. Ed.* **2003**, *42*, 1252-1255.

[4] (a) Ashe, A. J. III; Kampf, J. W.; Müller, C.; Schneider, M. *Organometallics* **1996**, *15*, 387-393. (b) Hoic, D. A.; DiMare, M.; Fu, G. C. *J. Am. Chem. Soc.* **1997**, *119*, 7155. (c) Ashe, A. J. III; Kampf, J. W.; Waas, J. R. *Organometallics* **1997**, *16*, 163-167. (d) Cui, P.; Chen, Y.; Wang, G.; Lu, G.; Xia, W. *Organometallics* **2008**, *27*. 4013-4016. (e) Yuan, Y.; Chen, Y.; Li, G.; Xia, W. *Organometallics* **2010**, *29*, 3722-3728. (f) In this species, the C-H in α of the B interacts with Yb: Cui, P.; Chen, Y.; Zhang, Q.; Li, G.; Xia, W. *J. Organomet. Chem.* **2010**, *695*, 2713-2719.

[5] Languérand, A.; Barnes, S. S.; Bélanger-Chabot, G.; Maron, L.; Berrouard, P.; Audet, P.; Fontaine, F.-G. *Angew. Chem., Int. Ed.* **2009**, *48*, 6695–6698.

[6] Barnes, S. S.; Légaré, M.-A.; Maron, L.; Fontaine, F.-G. *Dalton Trans.* **2011**, *40*, 12439-12442.

[7] Hoic, D. A.; Davis, W. M.; Fu, G. C. *J. Am. Chem. Soc.* **1996**, *118*, 8176-8177.

[8] (a) Hoic, D. A.; DiMare, M.; Fu, G. C. *J. Am. Chem. Soc.* **1997**, *119*, 7155-7156. (b) Bélanger-Chabot, G.; Rioux, P.; Maron, L.; Fontaine, F.-G. *Chem. Commun.*, **2010**, *46*, 6816–6818.

[9] The DPB was shown to be less donating than classical phosphide ligands (-PPh_2), but in the latter case, there is an additional lone pair on the phosphorus that can contribute electronically as well. See ref. 7.

[10] Gusev, D. G. *Organometallics* **2009**, *28*, 763-770.

[11] Herberich, G. E.; Becker, H. J.; Carsten, K.; Engelke, C.; Koch, W. *Chem. Ber.* **1976**, *109*, 2382-2388.

[12] E. Raabe, Dissertation, Rheinisch-Westfälische Technische Hochschule, Aachen (1984).

[13] Herberich, G. E.; Becker, H. J.; Hessner, B.; Zelenka, L. *J. Organomet. Chem.* **1985**, *280*, 147-151.

[14] (a) Barnett, B. L.; Krüger, C.; Tsay, Y. H. *Chem. Ber.* **1977**, *110*, 3900-3909. (b) Jones, R. A.; Stuart, A. L.; Atwood, J. L.; Hunter, W. E.; Rogers, R. D. *Organometallics* **1982**, *1*, 1721-1723. (c) Hanko, R. *Angew. Chem. Int. Ed. Engl.* **1985**, *24*, 704-705. (d) Tenorio, M. J.; Puerta, M. C.; Valerga, P. *J. Chem. Soc. Dalton Trans.* **1996**, 1305-1308. (e) Fryzuk, M. D.; Clentsmith, G. K. B.; Leznoff, D. B.; Rettig, S. J.; Geiib, S. J. *Inorg. Chim. Acta* **1997**, *265*, 169 – 177. (f) Kriley, C. E.; Woolley, C. J.; Krepps, M. K.; Popa, E. M.; Fanwick, P. E.; Rothwell, I. P. *Inorg. Chim. Acta* **2000**, *300–302*, 200-205. (g) Chen, Y.; Sui-Seng, C.; Zargarian, D. *Angew. Chem. Int. Ed.* **2005**, *44*, 7721-7725.

[15] Zhao, X.; Otten, E.; Song, D.; Stephan, D. W. *Chem. Eur. J.* **2010**, *16*, 2040-2044.

[16] (a) Kolpin, D. B.; Emslie, D. J. H. *Angew. Chem. Int. Ed.* **2010**, *49*, 2716-2719. (b) Emslie, D. J. H.; Harrington, L. E.; Jenkins, H. A.; Robertson, C. M.; Britten, J. F. *Organometallics* **2008**, *27*, 5317-5325.

[17] Herberich, G. E.; Englert, U.; Fischer, A.; Ni, J.; Schmitz, A. *Organometallics* **1999**, *18*, 5496-5501.

[18] (a) Hoic, D. A.; Wolf, J. R.; Davis, W. M.; Fu, G. C. *Organometallics* **1996**, *15*, 1315-1318. (b) Cade, I. A.; Hill, A. F. *Organometallics* **2012**, *31*, 2112-2115.

[19] Drew, D.; Doyle, J. R. *Inorganic Synthesis* **1990**, *28*, 346-349.

[20] Bruker. APEX 2 Version 2.0.2. *Bruker* AXS Inc., Madison, Wisconsin, USA, 2005.

[21] Bruker. SAINT Version 7.07a. *Bruker* AXS Inc., Madison, Wisconsin, USA, 2003.

[22] G. M. Sheldrick. SADABS Version 2004/1. *Bruker* AXS Inc., Madison, Wisconsin, USA, 2004.

[23] G. M. Sheldrick. Acta. Cryst. 2010, **A64**, 112-122.

[24] Gaussian 03, Revision C.02, M. J. Frisch, G. W. Trucks, H. B. Schlegel, G. E. Scuseria, M. A. Robb, J. R. Cheeseman, J. A. Montgomery, Jr., T. Vreven, K. N. Kudin, J. C. Burant, J. M. Millam, S. S. Iyengar, J. Tomasi, V. Barone, B. Mennucci, M. Cossi, G. Scalmani, N. Rega, G. A. Petersson, H. Nakatsuji, M. Hada, M. Ehara, K. Toyota, R. Fukuda, J. Hasegawa, M. Ishida, T. Nakajima, Y. Honda, O. Kitao, H. Nakai, M. Klene, X. Li, J. E. Knox, H. P. Hratchian, J. B. Cross, V. Bakken, C. Adamo, J. Jaramillo, R. Gomperts, R. E. Stratmann, O. Yazyev, A. J. Austin, R. Cammi, C. Pomelli, J. W. Ochterski, P. Y. Ayala, K. Morokuma, G. A. Voth, P. Salvador, J. J. Dannenberg, V. G. Zakrzewski, S. Dapprich, A. D. Daniels, M. C. Strain, O. Farkas, D. K. Malick, A. D. Rabuck, K. Raghavachari, J. B. Foresman, J. V. Ortiz, Q. Cui, A. G. Baboul, S. Clifford, J. Cioslowski, B. B. Stefanov, G. Liu, A. Liashenko, P. Piskorz, I. Komaromi, R. L. Martin, D. J. Fox, T. Keith, M. A. Al-Laham, C. Y. Peng, A. Nanayakkara, M. Challacombe, P. M. W. Gill, B. Johnson, W. Chen, M. W. Wong, C. Gonzalez, and J. A. Pople, Gaussian, Inc., Wallingford CT, 2004.

[25] Adamo, C.; Barone, V. *J. Chem. Phys.* **1998**, *108*, 664-675.

[26] (a) McLean, A. D.; Chandler, G. S. *J. Chem. Phys.* **1980**, *72*, 5639-5648. (b) Krishnan, R.; Binkley, J. S.; Seeger, R.; Pople, J. A. *J. Chem. Phys.* **1980**, *72*, 650-654. (c) Clark, T.; Chandrasekhar, J.; Spitznagel, G. W.; Schleyer, P. b. R. *J. Comp. Chem.* **1983**, *4*, 294-301. (d) Wachters, A. J. H. *J. Chem. Phys.* **1970**, *52*, 1033-1036. (e) Hay, P. J. *J. Chem. Phys.* **1977**, *66*, 4377-4384. (f) Frisch, M. J.; Pople, J. A.; Binkley, J. S. *J. Chem. Phys.* **1984**, *80*, 3265-3269.

[27] (a) Csaszar, P.; Pulay, P. *J. Mol. Struct.* **1984**, *114*, 31-34. (b) Farkas, Ö. PhD (CsC) thesis, Eötvös Loránd University and Hungarian Academy of Sciences, Budapest, **1995. (**c) Farkas, Ö.; Schlegel, H. B. *J. Chem Phys*. **1999**, *111*, 10806-10814.

[28] (a) Andrae, D.; Haeussermann, U.; Dolg, M.; Stoll, H.; Preuss, H. *Theor. Chim. Acta*, **1990**, *77*, 123. (b) Dolg, M.; Wedig, U.; Stoll, H.; Preuss, H. *J. Chem. Phys*. **1987**, *86*, 866. (c) Bergner, A.; Dolg, M.; Kuechle, W.; Stoll, H.; Preuss, H. *Mol. Phys.* **1993**, *80*, 1431-1441.

[29] (a) Maron, L.; Eisenstein, O. *J. Phys. Chem. A,* **2000**, *104*, 7140-7143. (b) Ehlers, A. W.; Böhme, M.; Dapprich, S.; Gobbi, A.; Höllwarth, A.; Jonas, V.; Köhler, K. F.; Stegmann, R.; Veldkamp, A.; Frenking, G. *Chem. Phys. Lett*. **1993**, *208*, 111-114.

[30] Hehre, W. J.; Ditchfield, R.; Pople, J. A. *J. Chem. Phys.* **1972**, *56*, 2257-2261.

[31] (a) Perdew, J. P.; Wang, Y. *Phys. Rev. B* **1992**, *45*, 284. (b) Becke, A. D. *J. Chem. Phys.* **1993**, *98*, 5648-5652.

[32] Reed, A. E.; Curtiss, L. A.; Weinhold, F. *Chem. Rev.*, **1988**, *88*, 899-926.